from the metal site upon inhibitor binding[34]). In Cd-substituted CPA, the Cd^{2+} is liganded by two histidines, a bidentate glutamate, and a water molecule. If one forms a plane that contains the Cd^{2+} and the two directly bonded nitrogen atoms from the histidines, then we have predicted[33] that σ_{33} will be nearly perpendicular to this plane, whereas σ_{11} is predicted to be nearly perpendicular to the plane of the bidentate glutamate or the water oxygen–Cd^{2+} bond. Therefore, due to the sensitivity of the shielding tensor elements to their orthogonal environments, σ_{11} and σ_{33} will be sensitive to the changes in the current density at the Cd^{2+}. Hence, if water is displaced (or not) upon inhibitor binding, this fact should be reflected in the NMR line shape for the Cd^{2+} nucleus. Further discussion about the orientation of the ^{113}Cd shielding tensor for this model compound in relation to Cd-substituted carboxypeptidase-A is addressed elsewhere.[33]

Acknowledgment. This work was partially supported by grants from the National Institutes of Health, GM 26295 and MARC predoctoral fellowship GM-09585 (E.R.). Many of the calculations discussed here were performed on a Microvax II computer obtained via an award from NSF, CHE86-13421. We also thank Dr. Shen-il Cho for his assistance in the electronic aspects of the single-crystal experiments. We also thank Dr. E. L. Amma of the Chemistry Department of the University of South Carolina for the use of the X-ray camera equipment necessary for the crystal alignment.

Supplementary Material Available: Tables containing details of the structure determination and refinement, anisotropic thermal parameters, bond distances and angles, and hydrogen atom positions for $Cd(OAc)_2(Im)_2$ (4 pages). Ordering information is given on any current masthead page.

(33) Rivera, E.; Kennedy, M. A.; Ellis, P. D. *Adv. Magn. Reson.* Academic Press: 1989; Vol. 13, pp 257-273.

(34) Mock, W. L.; Tsay, J.-T. *J. Am. Chem. Soc.* **1989**, *111*, 4467.

Why Is SiH_5^- a Stable Intermediate while CH_5^- Is a Transition State? A Quantitative Curve Crossing Valence Bond Study

Gjergji Sini,[1a] Gilles Ohanessian,[1a] Philippe C. Hiberty,*[1a] and Sason S. Shaik*[1b]

Contribution from the Laboratoire de Chimie Théorique,† Bât. 490, Université de Paris-Sud, 91405 Orsay Cedex, France, and the Department of Chemistry, Ben-Gurion University of the Negev, Beer-Sheva, 84105, Israel. *Received September 12, 1988*

Abstract: Valence bond computations of curve-crossing diagrams reveal a fundamental difference between the title species. The stability of SiH_5^- does not derive from hypervalency associated with d-AOs on Si but rather from the ability of Si to utilize its Si–H σ^* orbitals for bonding, much more so than C does with its σ^*(C–H) orbitals. Consequently, SiH_5^- possesses *two* resonating H--Si--H axial bonds; one via the axial p-AO of Si and the other via the equatorial $\sigma^*(SiH_3)$ orbital of the central SiH_3 fragment. As a result of the bonding capability of $\sigma^*(SiH_3)$, SiH_5^- can delocalize efficiently the fifth valence-electron pair into the equatorial Si–H bonds. The energy of SiH_5^- is thus lowered by the delocalization relative to $SiH_4 + H^-$. No significant stretching of the axial bonds is required to achieve this delocalized state, and therefore the bond lengths of SiH_5^- do not exceed those of SiH_4 by much. On the other hand, the $\sigma^*(CH_3)$ orbital possesses no bonding capability. The analogous delocalization of the fifth valence-electron pair is prohibited by the high promotion energy $p \rightarrow \sigma^*$ and by the nearly zero overlap of $\sigma^*(CH_3)$ with the axial hydrogens. As an alternative, CH_5^- localizes its fifth valence electron into the axial H--C--H linkage. This option leads to a long H--C--H linkage and a high energy of CH_5^- relative to $CH_4 + H^-$.

A fundamental chemical phenomenon is the different nature of the S_N2-type reactions at carbon and silicon.[2] This difference is exemplified in the simplest of these reactions, the H- exchange in eqs 1 and 2.[3]

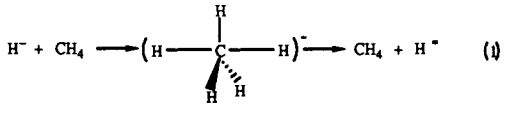

(1)

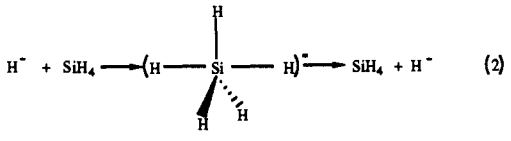

(2)

These two reactions are isoelectronic in terms of valence electrons and isostructural in terms of the geometric types of the main species along the reaction coordinate. Despite these similarities, the two reactions are quantitatively different. Thus, in reaction 1, the trigonal-bipyramidal CH_5^- is a high-energy transition state,[3,4] lying some 52–64 kcal/mol above the reactants and products, depending on the level of calculation. On the other hand, in reaction 2 the trigonal bipyramidal structure, recently synthesized and characterized in a gas-phase reaction,[5] is an intermediate,[3,4b,c,5-8] 13–20 kcal/mol lower than reactants and products, depending on the method of estimation.[4b,6-8]

What is the origin of this qualitative difference between the S_N2 chemistries of carbon and silicon?[2-9] One possible explanation is the participation of d-orbitals which endow Si with aptitude for pentacoordination.[2c,4c,5] However, at least for SiH_5^-,

† The Laboratoire de Chimie Théorique is associated with the CNRS (URA 506).

(1) (a) Université de Paris-Sud. (b) Ben-Gurion University.
(2) (a) Corriu, R. J. P.; Dabosi, G.; Martineau, M. *J. Organomet. Chem.* **1980**, *186*, 25. (b) Stevenson, W. H.; Martin, J. C. *J. Am. Chem. Soc.* **1985**, *107*, 6352. (c) Corriu, R. J. P.; Guerin, C. *Adv. Organomet. Chem.* **1982**, *20*, 26. (d) Corriu, R. J. P.; Guerin, C. *J. Organomet. Chem.* **1980**, *198*, 231.
(3) Payzant, J. D.; Tanaka, K.; Betovski, L. D.; Bohme, D. K. *J. Am. Chem. Soc.* **1976**, *98*, 894.
(4) See for example: (a) Dedieu, A.; Veillard, A. *J. Am. Chem. Soc.* **1972**, *94*, 6730. (b) Baybutt, P. *Mol. Phys.* **1975**, *29*, 389. (c) Keil, F.; Ahlrichs, R. *J. Am. Chem. Soc.* **1972**, *94*, 6730. (d) Wolfe, S.; Mitchell, D. J.; Schlegel, H. B. *J. Am. Chem. Soc.* **1981**, *103*, 7694.
(5) Hajdasz, D. J.; Squires, R. R. *J. Am. Chem. Soc.* **1986**, *108*, 3139.
(6) Wilhite, D. L.; Spialter, L. *J. Am. Chem. Soc.* **1973**, *95*, 2100.
(7) Reed, A. E.; Schleyer, P. v. R. *Chem. Phys. Lett.* **1987**, *133*, 553.
(8) Keil, F.; Ahlrichs, R. *Chem. Phys.* **1975**, *8*, 384.
(9) For discussions see: Anh, N. T.; Minot, C. *J. Am. Chem. Soc.* **1980**, *102*, 103.

0002-7863/90/1512-1407$02.50/0

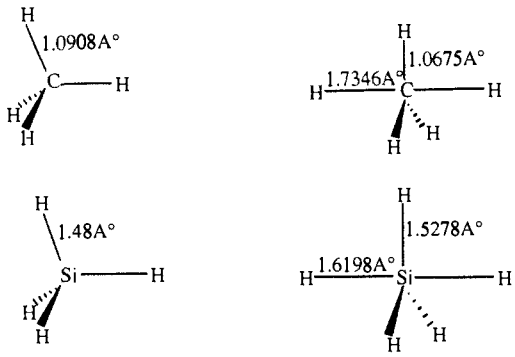

Figure 1. Geometries of MH_4 and MH_5^- (M = C, Si) species from ref 4b.

the dominant role of d-orbitals has recently been ruled out by Reed and Schleyer,[7] who have shown SiH_5^- to be more stable than $SiH_4 + H^-$ even in the absence of d-orbitals. This last finding makes the study of the bonding in CH_5^- and SiH_5^- fundamental to the understanding of the propensity of Si, in contrast to almost exclusive reluctance of C, for pentacoordination.[10]

Another intriguing problem derives from the structural differences between CH_5^- and SiH_5^- and may be related to their different bonding properties. Figure 1 displays the structures computed by Baybutt.[4b] Thus, in CH_5^- the axial bonds are much longer (by more than 60%) than both the equatorial bonds and the C–H bonds of the parent molecule, CH_4. On the other hand, in SiH_5^-, the lengths of the axial and equatorial bonds are similar and only slightly longer (3–9%) than the Si–H bond of SiH_4. It appears therefore that generating CH_5^- from $H^- + CH_4$ requires, in addition to the flattening of the CH_3 angle in CH_4, a very extensive amount of bond stretching. On the other hand, generating SiH_5^- from its constituents requires mainly the angular deformation, with little bond elongation. Moreover, in SiH_5^- both axial and equatorial bonds are participating in the bond elongation deformation, while in CH_5^- only the axial bonds are significantly stretched.

Thus, the difference between reactions 1 and 2 is both in their energetic behavior, along the reaction coordinate, and in the deformation features of the MH_5^- (M = C, Si) species, relative to their parent MH_4 molecules. These two types of qualitative differences may be linked and reflect different bonding mechanisms in the two species, and this is the insight we try to provide in this paper.

To gain this insight we use the valence bond (VB) model of curve crossing[11,12] which has been applied qualitatively to discuss similar problems, in carbon S_N2 reactivity,[13] and in the stability patterns of delocalized X_n (n = 3, 4, 6) clusters.[14] In this manuscript, the model is applied quantitatively[15] in order to anchor the qualitative insight on a sound computational basis.

The first section of the paper reviews briefly the main elements of the curve-crossing model. The second section discusses computational details of the VB method, which is used to generate the curves. This is followed by sections that discuss the quantitative curve-crossing diagrams for reactions 1 and 2.

The Qualitative Curve-Crossing Model

The curve-crossing diagrams can be constructed from a minimal number of "effective"[16] VB configurations, which we hereafter call VB structures. These structures are shown in **1–4** with the trigonal-bipyramidal geometry as an example. The dots represent electrons, the lines represent bonds, while H_l and H_r are the left- and right-hand-side axial hydrogens that are interchanging during the reaction. Structures **1** and **2** are the two Lewis structures

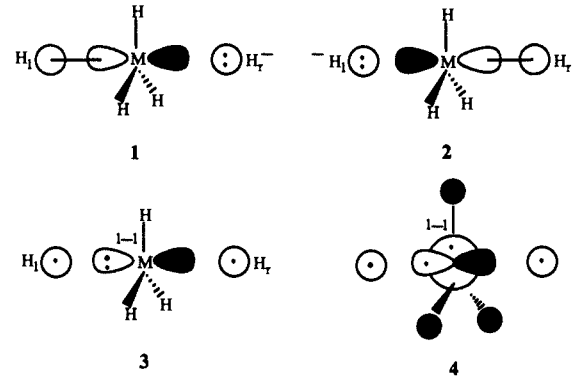

that describe the two-electron pairs of the two "active" bonds that are broken and made during the reaction. Each Lewis structure, by itself, is made up of an optimized mixture of a Heitler–London (HL) and two ionic configurations, which are exemplified in **5–7** for the H_l–M Lewis structure **1**. The spin pairing in **5** is indicated by a line connecting the two dots.

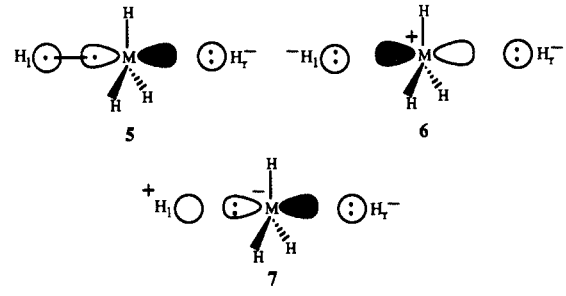

If the negative charge is now located on the MH_3 fragment, two alternatives are possible: (i) In structure **3** the axial orbital of the MH_3 fragment is doubly occupied. It is a long bond structure which possesses two singlet-paired electrons on the two axial hydrogens. (ii) In structure **4** the negative charge of the central fragment is now delocalized over the three M–H linkages. It involves one electron occupying the axial AO and another electron in a $\sigma^*(MH_3)$ orbital of a_1 symmetry (a'_1 when MH_3 is planar). This configuration is equivalent to resonating mixture **8**, with an electron allowed to occupy each of the localized σ^* bond orbitals of the three equatorial bonds of the central MH_3 unit. Of course, the lowest energy for this structure is obtained if the four odd electrons can be paired up efficiently into two bond pairs.

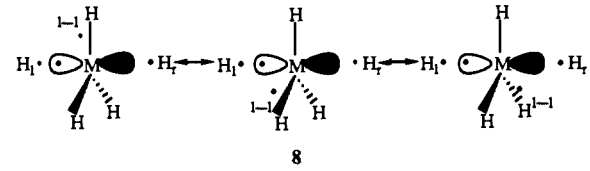

Both structures **3** and **4** are essential because they mix the two Lewis structures at any point along the reaction coordinate, other than the two ground states.[11,13]

We can now use this minimal set of VB structures to construct the curve-crossing diagrams for reactions 1 and 2. Initially, one can generate two-curve[13,17] or many-curve[18,19] models. However,

(10) Two exceptions are discussed: (a) Forbus, T. R., Jr.; Martin, J. C. *J. Am. Chem. Soc.* **1979**, *101*, 5057. (b) Schleyer, P. v. R.; Würthwein, E. K.; Clark, T. *J. Am. Chem. Soc.* **1983**, *105*, 5930.

(11) Shaik, S. S. *J. Am. Chem. Soc.* **1981**, *103*, 3692.

(12) (a) Pross, A.; Shaik, S. S. *Acc. Chem. Res.* **1983**, *16*, 361. (b) For a recent review of the model see: Lowry, T. H.; Richardson, K. S. *Mechanism and Theory in Organic Chemistry*; Harper and Row: New York, 1987; pp 218–222, 354–360.

(13) Shaik, S. S. *Prog. Phys. Org. Chem.* **1985**, *15*, 197.

(14) (a) Shaik, S. S.; Hiberty, P. C.; Lefour, J.-M.; Ohanessian, G. *J. Am. Chem. Soc.* **1987**, *109*, 363. (b) Shaik, S. S.; Hiberty, P. C.; Ohanessian, G.; Lefour, J.-M. *J. Phys. Chem.* **1988**, *92*, 5086.

(15) For a related calculation see: Bernardi, F.; Robb, M. A. *J. Am. Chem. Soc.* **1984**, *106*, 54.

(16) (a) Shaik, S. S. In *New Concepts for Understanding Organic Reactions*; Bertran, J., Csizmadia, I. G., Eds.; Kluwer Publications: Dordrecht, 1989. (b) Reference 13, pp 284–285.

(17) Sini, G.; Shaik, S. S.; Lefour, J.-M.; Ohanessian, G.; Hiberty, P. C. *J. Phys. Chem.* **1989**, *93*, 5661.

(18) See p 205 in ref 13.

(19) Pross, A. *Adv. Phys. Org. Chem.* **1985**, *21*, 99 (especially p 125).

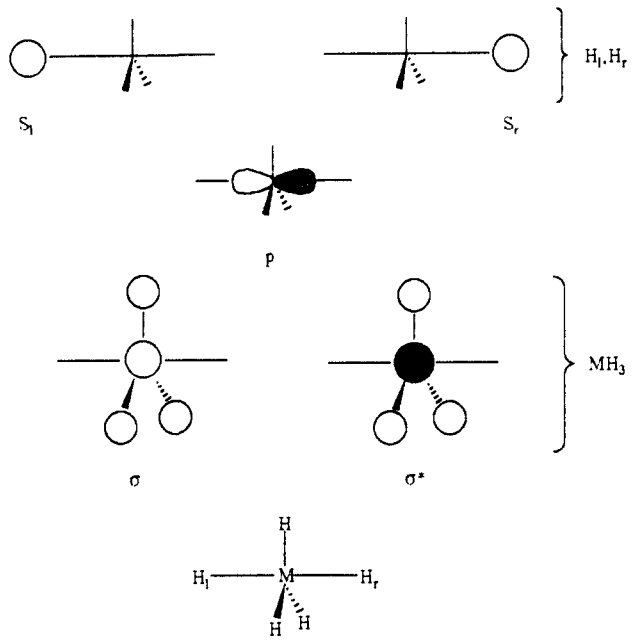

Figure 2. Elementary valence orbitals for the H_l, H_r, and MH_3 fragments of the MH_5^- structure. The π-type orbitals of the central MH_3 fragment are not shown.

since we have discovered (vide infra) that structure **4** is responsible for the intermediacy of SiH_5^- in reaction 2, we prefer to treat each structure (**1–4**) as an independent curve. The four-curve model is exemplified below for reaction 1 in Figure 3, where curves 1–4 correspond to the energy variation of structures **1–4**, respectively, along the unique points of the reaction coordinate.

Let us now describe the details of the quantitative calculations of the four curve models of reactions 1 and 2.

Theoretical Methods

Our computational method has been described in detail elsewhere[20,21] and tested for accuracy and only the basic principles will be recalled here. It is a nonorthogonal CI between valence bond functions (VBFs) in which atomic orbitals or fragment orbitals (FOs) are spin-coupled so as to represent chemical structures. The truncation of the CI is based on two principles: (i) Only the electrons corresponding to the "active bonds", i.e. the bonds that are broken or made throughout the reaction process, are correlated. The other electrons, namely the core electrons and those involved in the "inactive bonds", i.e. the three M–H bonds of the MH_3 fragment, are frozen into doubly occupied SCF MOs. This principle is similar to the OVC treatment of Das and Wahl,[22] or to the CCCI of Carter and Goddard.[23] (ii) A VB wave function is supposed to be energetically reliable if it involves all relevant chemical structures (here the neutral and ionic components of **1–4**) and if each one of them is optimally described, i.e. by a single VBF constructed out of FOs optimized for this particular VBF.

The second principle can be satisfied in two ways: (i) Only one VBF per chemical structure may be included in the CI, and each VBF is allowed to have its own set of orbitals, different from one VBF to the other. The inconvenience of this technique is that one may have to deal with a very large number of orbitals when the wave function is composed of many resonance structures. (ii) One VBF per chemical structure is generated out of a common set of low-energy FOs (hereafter called elementary FOs) arising from, e.g., SCF calculations on the isolated fragments H_l, CH_3, and H_r. To these "elementary" VBFs, we add in the CI "complementary" VBFs, generated from the elementary ones by replacing elementary FOs by virtual ones. Thus, each chemical structure is represented by several VBFs, and the complementary VBFs are systematically generated and chosen so as to correct for the possible inadequacy of the elementary FOs, which are optimized for isolated fragments, as regards hybridization, polarization, and orbital diffuseness.

The elementary FOs of H_l and H_r are called s_l and s_r, respectively; p, σ, and σ^* respectively represent the axial orbital and the bonding and antibonding orbitals of a_1 symmetry of the central fragment, MH_3. These orbitals are illustrated in Figure 2, in the geometry of the symmetrical MH_5^- complex.

The elementary FOs are SCF optimized at each calculated point of the potential surface, so as to allow the MH_3 fragment to follow the distortions of the supersystem. The virtual orbitals carry the same labels but with a prime. It is important to emphasize that the FOs of each VBF have no delocalization tails on other fragments, as opposed to other methods such as GVB[24] or SCVB.[25] This makes the VB configurations the closest possible to the chemical structures used in qualitative discussions.[26] To better understand the role of d-orbitals, we have performed the VB calculations with two basis sets: with and without d-orbitals on the central atom. For computational convenience, we have chosen the smallest possible basis sets still yielding reasonable energetics at the Hartree–Fock level. The 6-31G+D and 6-31G*+D basis sets,[27] where D refers to diffuse orbitals of exponent 0.036 on the axial hydrogens, proved to be a good compromise.

So defined, the complete set of VBFs adds to a total of 219 with 6-31G+D basis set and 304 with 6-31G*+D, for both CH_5^- and SiH_5^-, and throughout the reaction coordinate (complex, reactants and products). Now some VBFs have been discarded from the aboved-defined set, for the sake of reducing computer time, after some computational tests showing that this simplification had no important effect on the calculated energies: (i) H^-, in reactants and products, is described by only two VBFs, s^2 and ss'. A full CI calculation on H^- shows that this results in a difference of only 1 kcal/mol. (ii) The effect of diffuse orbitals can be shown by SCF calculations to be negligible (less than 2 kcal/mol) in the SiH_5^- intermediate. The corresponding complementary VBFs have been removed. (iii) With use of the fact that structure **4** is an important one in the SiH_5^- (see below), it has been possible to get optimal σ and σ^* AOs for this structure from the $3a_1'$ and $4a_1'$ SCF MOs of the D_{3h} intermediate (which are mainly localized on the Si–H equatorial bonds), after dropping their axial hydrogen components and renormalizing, thus rending complementary VBFs unnecessary. (iv) Lastly, the VBFs that proved inefficient with 6-31G+D have been removed before using the largest 6-31G*+D basis set. This results in an energy rise less than 1 kcal/mol. The VBFs that are kept after these simplifications are displayed in Table I for D_{3h} CH_5^- and Table II for D_{3h} SiH_5^-, with their coefficients in the ground state, as calculated with the 6-31G+D basis set. The CI lists add to 138 and 133 configurations, respectively, versus 174 and 169 with the 6-31G*+D basis set.

All the above VBF types are used also for the calculation of the reactants and products.

Results

A. Adiabatic Ground-State Surfaces. Comparison with Previous Works. A number of theoretical studies of CH_5^- and SiH_5^- have been published.[4,6–9,28] At the SCF level, CH_5^- is found to be higher in energy than $H^- + CH_4$ by 61.2–63.6 kcal/mol. SiH_5^- on the other hand is calculated to be below $H^- + SiH_4$ by 13.1–18.6 kcal/mol,[4b,c,7] the most recent SCF value being the former.[7] By using the CEPA method[29] the barrier for reaction 1 is reduced by 7.2 kcal/mol[8] and the potential well for reaction 2 is deepened by 6.3 kcal/mol.[8] A recent calculation[7] of reaction 2 by means of the MP4 method, with the 6-31++G** basis set, estimates the electron correlation effect as 5.0 kcal/mol. Our own SCF and VB calculations are displayed in Table III.

(20) Hiberty, P. C.; Lefour, J.-M. *J. Chim. Phys.* **1987**, *84*, 607.
(21) Maitre, P.; Lefour, J.-M.; Ohanessian, G.; Hiberty, P. C. *J. Phys. Chem.*, in press.
(22) (a) Das, G.; Wahl, A. C. *J. Chem. Phys.* **1967**, *47*, 2934. (b) *Ibid.* **1972**, *56*, 1769, 3532. (c) Stevens, W. J.; Das, G.; Wahl, A. C.; Krauss, M.; Neumann, D. *Ibid.* **1974**, *61*, 3686.
(23) Carter, E. A.; Goddard, W. A., III *J. Chem. Phys.* **1988**, *88*, 3132.
(24) Bobrowicz, F. B.; Goddard, W. A., III In *Methods of Electronic Structure Theory*; Schaefer, H. F., Ed.; Plenum: New York, 1977; pp 79–127.
(25) Cooper, D. L.; Gerratt, J.; Raimondi, M. *Adv. Chem. Phys.* **1987**, *59*, 319.
(26) Ohanessian, G.; Hiberty, P. C. *Chem. Phys. Lett.* **1987**, *137*, 437.
(27) For first row elements: Hehre, W. J.; Ditchfield, R.; Pople, J. A. *J. Chem. Phys.* **1972**, *56*, 2257. Hariharan, P. C.; Pople, J. A. *Theor. Chim. Acta (Berlin)* **1973**, *28*, 213. For second row elements: Francl, M. M.; Pietro, W.; Hehre, W. J.; Binkley, J. S.; Gordon, M. S.; DeFrees, D. J.; Pople, J. A. *J. Chem. Phys.* **1982**, *77*, 3654. Gordon, M. S.; Binkley, J. S.; Pople, J. A.; Pietro, W. J. *J. Am. Chem. Soc.* **1982**, *104*, 2797.
(28) For additional extended basis set computations of $H^- + CH_4$ see: (a) Leforestier, C. *J. Chem. Phys.* **1978**, *68*, 4406. (b) Dedieu, A.; Veillard, A.; Roos, B. *Proceedings of the 6th Jerusalem Symposium on Quantum Chemistry*; Israel Academy of Science: Jerusalem, 1974. (c) Cremer, D.; Kraka, E. *J. Phys. Chem.* **1986**, *90*, 33. (d) Kost, D.; Aviram, K. *Tetrahedron Lett.* **1982**, *23*, 4157. (e) Ritchie, C. D.; Chappell, G. A. *J. Am. Chem. Soc.* **1970**, *92*, 1819.
(29) Kutzelnigg, W. In *Methods of Electronic Structure Theory*; Schaefer, H. F., Ed.; Plenum: New York, 1977; pp 160–182.

Table I. VBFs Used for the 6-31G+D Calculation of the Adiabatic[a,b] CH_5^- and Its Diabatic Components

structure	type	VBF[c]	coefficient
covalent **1**[d]		$s_l s_r^2 p\sigma^2$	0.1156
		$s_l' s_r^2 p\sigma^2$	0.0140
		$s_l s_r s_r' p\sigma^2$	0.0199[f]
		$s_l s_r s_r'' p\sigma^2$	0.4483[f]
		$s_l s_r'^2 p\sigma^2$	0.0144
		$s_l' s_r s_r' p\sigma^2$	0.0021[f]
		$s_l' s_r s_r'' p\sigma^2$	0.0044[f]
		$s_l' s_r'^2 p\sigma^2$	0.0015
		$s_l s_r^2 p'\sigma^2$	0.0089
		$s_l s_r s_r' p'\sigma^2$	0.0097[f]
		$s_l s_r s_r'' p'\sigma^2$	0.0159[f]
		$s_l s_r'^2 p'\sigma^2$	0.0026
		$s_l' s_r^2 p'\sigma^2$	0.0029
ionic	**1**[e]	$s_r^2 p^2\sigma^2$	0.0171
		$s_r s_r'' p^2\sigma^2$	0.0270
		$s_r^2 pp'\sigma^2$	0.0104
		$s_r s_r'' pp'\sigma^2$	0.0125[f]
		$s_l^2 s_r^2\sigma^2$	0.0720
		$s_l^2 s_r s_r'\sigma^2$	0.0080
		$s_l^2 s_r s_r''\sigma^2$	0.1804
		$s_l^2 s_r'^2\sigma^2$	0.0226
		$s_l s_l' s_r s_r'\sigma^2$	0.0042[f]
		$s_l s_l'' s_r s_r''\sigma^2$	0.0931[f]
		$s_l^2 s_r^2\sigma\sigma^*$	0.0036
		$s_l s_l'' s_r^2\sigma\sigma^*$	0.0950
	3	$s_l s_r p^2\sigma^2$	0.0054
		$s_l s_r pp'\sigma^2$	0.0406[f]
		$s_l s_r' p^2\sigma^2$	0.0130
		$s_l s_r' pp'\sigma^2$	0.0037[f]
		$s_l s_r p^2\sigma\sigma^*$	0.1938[f]
covalent	**4**	$s_l s_r p\sigma^2\sigma^*$	0.1685[f]
		$s_l s_r p\sigma^2\sigma^{*\prime}$	0.0447[f]
		$s_l s_r p'\sigma^2\sigma^{*\prime}$	0.0055[f]
		$s_l' s_r p\sigma^2\sigma^*$	0.0031[f]
		$s_l s_r' p\sigma^2\sigma^{*\prime}$	0.0052[f]
		$s_l' s_r p'\sigma^2\sigma^*$	0.0010[f]
		$s_l' s_r' p\sigma^2\sigma^*$	0.0009[f]
ionic	**4**	$s_l s_r^2\sigma^2\sigma^*$	0.0288
		$s_l' s_r^2\sigma^2\sigma^*$	0.0004
		$s_l s_r s_r'\sigma^2\sigma^*$	0.0065[f]
		$s_l s_r s_r''\sigma^2\sigma^*$	0.0219[f]
		$s_l s_r^2\sigma^2\sigma^{*\prime}$	0.0177
		$s_l' s_r^2\sigma^2\sigma^{*\prime}$	0.0045
		$s_l' s_r s_r'\sigma^2\sigma^*$	0.0003[f]
		$s_l' s_r s_r''\sigma^2\sigma^*$	0.0030[f]
		$s_l s_r s_r'\sigma^2\sigma^{*\prime}$	0.0025[f]
		$s_l s_r s_r''\sigma^2\sigma^{*\prime}$	0.0024[f]
		$s_r^2 p\sigma^2\sigma^*$	0.0074
		$s_r s_r'' p\sigma^2\sigma^*$	0.0151[f]

[a] The coefficients in the table are results for the adiabatic CH_5^-. [b] In each case we show only one of the two symmetry related VBFs (e.g., **1** instead of **1** and **2**). [c] The primed orbitals correspond to the virtual SCF orbitals of the fragments. s_l'' and s_r'' are the diffuse orbitals on the left and right hydrogens, respectively. [d] This corresponds to drawing **5** in the text. [e] This corresponds to drawing **6** or **7** in the text. [f] In this VBF both spin coupling schemes have been used but only the largest coefficient is shown.

The VB computed barriers of reaction 1 are lower than the SCF ones by 6.9 kcal/mol, which is the expected electron correlation according to Keil and Ahlrichs.[8] The expected correlation effect is observed also for reaction 2 as can be seen from the VB computed energy well being 4.0–5.8 kcal/mol deeper than the SCF one.

B. Quantitative Four-Curve Models for Reactions 1 and 2. Reaction 1. The four-curve diagram, calculated with the 6-31G*+D basis set, is displayed in Figure 3. It appears that structures **1** and **2** contribute most to the adiabatic ground-state surface, as expected. Structures **3** and **4** have only a corrective role, but they are not negligible since the energy barrier is calculated to be 71.5 kcal/mol if **3** and **4** are discarded vs 56.8 kcal/mol if they are included.

Reaction 2. To better illustrate the reason for the stability of the SiH_5^- complex even in the absence of d-orbitals on silicon,

Table II. VBFs Used for the 6-31G+D Calculation of the Adiabatic SiH_5^- Complex[a,b]

structure	type[c]	coefficient	coefficient
covalent	**1**[d]	$s_l s_r^2 p\sigma^2$	0.2335
		$s_l' s_r^2 p\sigma^2$	0.0092
		$s_l s_r s_r' p\sigma^2$	0.0746[f]
		$s_l s_r'^2 p\sigma^2$	0.0204
		$s_l' s_r'^2 p\sigma^2$	0.0002
		$s_l s_r^2 p'\sigma^2$	0.0877
		$s_l s_r s_r' p'\sigma^2$	0.0129[f]
		$s_l s_r'^2 p'\sigma^2$	0.0066
		$s_l' s_r^2 p'\sigma^2$	0.0058
ionic	**1**[e]	$s_r^2 p^2\sigma^2$	0.0095
		$s_r pp'\sigma^2$	0.0061
		$s_l^2 s_r^2\sigma^2$	0.1507
		$s_l^2 s_r s_r'\sigma^2$	0.0361
		$s_l^2 s_r'^2\sigma^2$	0.0231
		$s_l s_l' s_r s_r'\sigma^2$	0.0158[f]
		$s_l^2 s_r^2\sigma\sigma^*$	0.0372
		$s_l^2 s_r s_r'\sigma\sigma^*$	0.0542[f]
	3	$s_l s_r p^2\sigma^2$	0.0128
		$s_l s_r pp'\sigma^2$	0.0225[f]
		$s_l s_r' p^2\sigma^2$	0.0073
		$s_l s_r' pp'\sigma^2$	0.0075
		$s_l s_r p^2\sigma\sigma^*$	0.2199[f]
		$s_l s_r' p^2\sigma\sigma^*$	0.0315[f]
covalent	**4**	$s_l s_r p\sigma^2\sigma^*$	0.2679[f]
		$s_l s_r p'\sigma^2\sigma^*$	0.1039[f]
		$s_l s_r p\sigma\sigma^{*2}$	0.0876[f]
		$s_l s_r' p\sigma\sigma^{*2}$	0.0134[f]
		$s_l s_r p\sigma^2\sigma^{*\prime}$	0.0631
		$s_l s_r p'\sigma^2\sigma^{*\prime}$	0.0226[f]
		$s_l' s_r p\sigma^2\sigma^*$	0.0192[f]
		$s_l' s_r p\sigma^2\sigma^{*\prime}$	0.0130[f]
		$s_l' s_r p'\sigma^2\sigma^*$	0.0103[f]
ionic	**4**	$s_l' s_r^2\sigma^2\sigma^*$	0.1331
		$s_l' s_r^2\sigma^2\sigma^*$	0.0017
		$s_l s_r s_r'\sigma^2\sigma^*$	0.0233[f]
		$s_l s_r^2\sigma^2\sigma^{*\prime}$	0.0428
		$s_l' s_r^2\sigma^2\sigma^{*\prime}$	0.0005
		$s_l' s_r s_r'\sigma^2\sigma^*$	0.0048[f]
		$s_l s_r s_r'\sigma^2\sigma^{*\prime}$	0.0114[f]
		$s_r^2 p\sigma^2\sigma^*$	0.0103
		$s_r s_r' p\sigma^2\sigma^*$	0.0137[f]
		$s_r p^2\sigma^2\sigma^*$	0.0130
		$s_r' p^2\sigma^2\sigma^*$	0.0101
		$s_r pp'\sigma^2\sigma^*$	0.0152[f]
		$s_r' pp'\sigma^2\sigma^*$	0.0025[f]

[a] The coefficients in the table are results for the adiabatic CH_5^-. [b] In each case we show only one of the two symmetry related VBFs (e.g., **1** instead of **1** and **2**). [c] The primed orbitals correspond to the virtual SCF orbitals of the fragments. s_l'' and s_r'' are the diffuse orbitals on the left and right hydrogens, respectively. [d] This corresponds to drawing **5** in text. [e] This corresponds to drawing **6** or **7** in the text. [f] In this VBF both spin coupling schemes have been used but only the largest coefficient is shown.

Table III. Total Energies (au) of Some Selected Points of the MH_5^- Potential Surfaces, As Calculated by the SCF and VB Methods (Reaction Barriers in kcal/mol)

	6-31G+D		6-31G*+D	
	SCF	VB	SCF	VB
$CH_4\cdots H^-$	−40.6675	−40.70323	−40.68151	−40.71582
CH_5^-	−40.56460	−40.61125	−40.57995	−40.62526
barrier for reaction 1	64.6	57.7	63.7	56.8
$SiH_4\cdots H^-$	−291.65900	−291.66935	−291.71075	−291.72597
SiH_5^-	−291.66194	−291.68144	−291.72618	−291.74788
barrier for reaction 2	−1.8	−7.6	−9.7	−13.7

we display the four-curve diagram of SiH_5^-, calculated with the 6-31G+D basis set, which only involves orbitals of s and p type (Figure 4).

It is immediately apparent that if only curves 1–3 were considered, the diagram would not be very different from that of CH_5^-

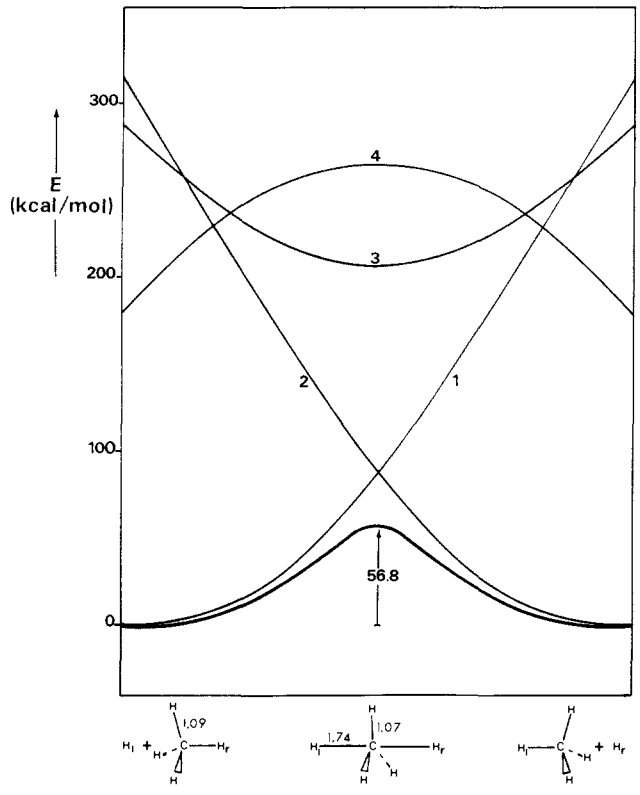

Figure 3. A four-curve avoided-crossing diagram for reaction 1. The adiabatic curve, which results from mixing **1**, **2**, **3**, and **4**, is shown by the heavy line. The values on the energy scale are computed with the VB method by use of the 6-31G*+D basis set.

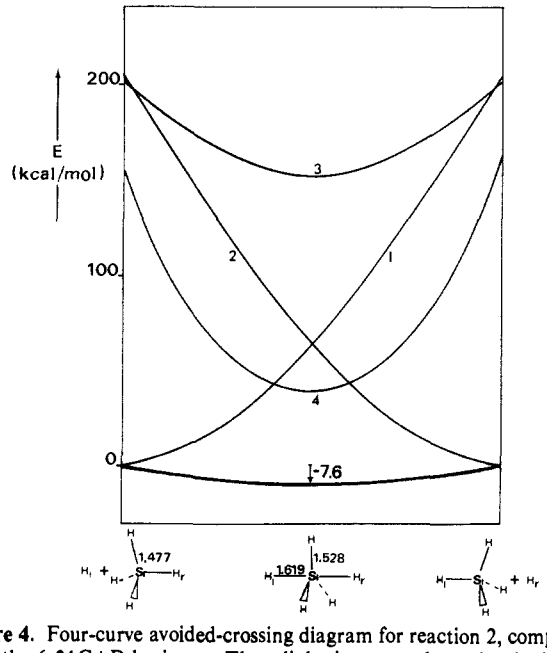

Figure 4. Four-curve avoided-crossing diagram for reaction 2, computed with the 6-31G+D basis set. The adiabatic curve, shown by the heavy line, is a result of mixing of **1**, **2**, **3**, and **4**.

in Figure 3. Indeed the energy of the SiH_5^- symmetrical complex, as computed by mixing together these three structures *only*, yields a barrier of 27 kcal/mol. *It is curve 4 that makes all the difference.* This curve begins as a high energy structure, ~153 kcal/mol above the reactants, and shoots down very steeply to become the lowest energy structure at the D_{3h} geometry.

The role of d-orbitals can be investigated in detail by using the 6-31G*+D basis set. Historically, the d-orbitals were believed to play the role of valence orbitals and to be responsible for the pentacoordination of SiH_5^- via an sp^3d-type hybridization in the silicon atom. The corresponding VB structure (hereafter called

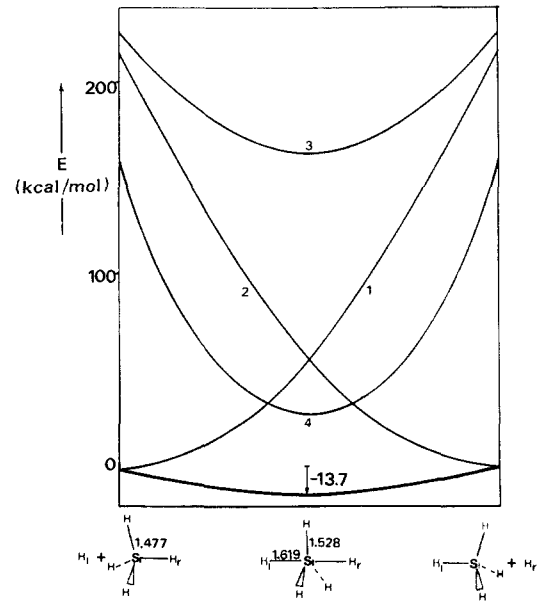

Figure 5. A four-curve avoided-crossing diagram for reaction 2 computed with the 6-31G*+D basis set.

sp^3d structure) is simply obtained from **4** by substituting σ^* for a d_{z^2} orbital.

As σ^* and d_{z^2} have the same symmetry properties, it may be anticipated that the structures sp^3d and **4** overlap each other, and that perhaps only one of them is necessary to account for the stability of SiH_5^-. This point can be most simply elucidated in the framework of VB theory, which allows the removal of structures **4** or sp^3d from the calculation. Thus, we have computed the energy of the SiH_5^- complex, with the 6-31G*+D basis set, by substituting σ^* for a d_{z^2} orbital in all the VB structures corresponding to **4** in Table II, thus estimating the effect of the sp^3d structure in the absence of **4**. We found a barrier of 14 kcal/mol in reaction 2. By comparison, the barrier calculated in the absence of d-orbitals *and* of structure **4** is 27 kcal/mol (vide supra). The stabilizing effect of the sp^3d structure can thus be estimated to be 13 kcal/mol. On the other hand, structure **4**, in the absence of d-orbitals, stabilizes SiH_5^- by 35 kcal/mol, to give an energy well 7.6 kcal/mol deep (Figure 4).

Lastly, if the sp^3d structure is mixed with structure **4** in the diagram, to constitute curve 4 as in Figure 5, the calculated well for reaction 2 gets deeper, down to −13.7 kcal/mol. The cumulated stabilizing effect of **4** and sp^3d is therefore ~41 kcal/mol, slightly less than the sum of their isolated effects. This shows that even though the effects of sp^3d and **4** are slightly redundant, it is the latter structure that is by far the most important and remains the central explanation for the stability of SiH_5^-, irrespective of the basis set.

Another interesting feature of the double-avoided crossing in Figures 4 and 5 is the possibility of observing small barriers for formation and decomposition of the SiH_5^- intermediate. Such bumps may result from the avoided crossing between curves 1 and 4 on the one hand and 2 and 4 on the other hand. In the very detailed theoretical study of reaction 2 by Reed and Schleyer,[7] no barrier is effectively observed but a trace of it is evidenced in the form of an inflexion point at an Si--H^- distance of 2.97 Å, followed by a flat region up to a distance of 3.2 Å.

Discussion: How Do SiH_5^- and CH_5^- Mutually Differ?

Structure **4** appears to be the key factor that differentiates SiH_5^- from CH_5^-. A few questions then arise: (a) Why does this structure become so stable in SiH_5^-? (b) How is this responsible for, or associated with, the different geometric features of CH_5^- or SiH_5^-? (c) What are the different bonding features of SiH_5^- and CH_5^-? We shall now try to provide this insight using the elements of the VB model.

A. Bonding Features of SiH_5^- and CH_5^-. Let us start with the bonding features of CH_5^- and SiH_5^- and construct them from a

central planar fragment MH_3^- and two axial atoms H_l and H_r. The choice of fragment charges will become clear as the discussion proceeds.

Bonds between two fragments are made by singlet pairing two odd electrons, one on each fragment. When a fragment has a closed shell ground state, the only way it can make bonds is by being promoted to an excited open-shell configuration. Forming such bonds requires the promotion energies to be low, and orbitals that can sustain large overlaps with other fragments' orbitals.

The closed shell MH_3^- fragment has two options to bind H_l and H_r. The first is by promoting one electron to the $\sigma^*(MH_3)$ orbital, as shown in **9**.

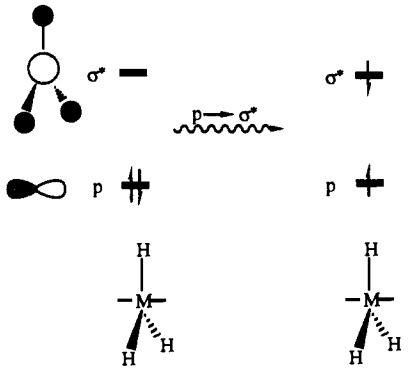

9

This generates an excited MH_3^- fragment that is prepared in principle for the formation of the two bonds. One bond utilizes the axial p-AO of the central fragment, and the other utilizes the $\sigma^*(MH_3)$ orbital, as shown in **10** and **11** with use of the usual overlap pictures of the orbital constituents to schematize a bond between two centers. In fact, because of the identical status of H_l and H_r, either one can sample the two bond types, and the picture will consist of resonating bond types. This bonding mechanism corresponds to structure **4**.

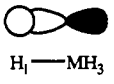

H_l—MH_3

10 (p-bond)

H_3M—H_r

11 (σ^*-bond)

The second bonding opportunity arises by transferring an electron from MH_3^- to one of the axial hydrogens, e.g. H_r. The remaining open-shell electrons, one in the axial p-AO of MH_3 and the other on the neutral hydrogen H_l, can now be paired into a resonating p-type bond, **10**. This bonding mechanism corresponds to structures **1** and **2**.

The importance of the p-bond (**10**), for both CH_3 and SiH_3, is not in doubt because the p-orbital is low lying and has a good overlap capability. But how and when does the σ^*-bond (**11**) become important?

First of all, the promotion energy $p \rightarrow \sigma^*$ (**9**) is 55 kcal/mol lower for SiH_3 relative to CH_3. Second, and perhaps more importantly, the overlap capability of $\sigma^*(MH_3)$ is very different for Si and C. Thus, for SiH_3 the σ^*–H_l (or σ^*–H_r) overlap is significant (0.175 in 6-31G basis set), while for CH_3 the same overlap is close to zero (0.037). The cause will be immediately exposed, but it is already apparent that $\sigma^*(SiH_3)$ has a significant bonding capability, of which $\sigma^*(CH_3)$ is devoid. Therefore, SiH_5^- can utilize two bonds (**10** and **11**) to bind SiH_3 to H_l and H_r, and this is the reason for the low energy of structure **4** in Figure 4, at the trigonal-bipyramidal geometry. On the other hand, the almost zero overlap capability of $\sigma^*(CH_3)$ prohibits the stabilization of **4**, which remains high in energy, as shown in Figure 3. The very same reasons, high energy and poor overlap capability of $\sigma^*(CH_3)$, diminish the mixing of **4** into **1** and **2**. The net effect is that the main bonding mechanism in CH_5^- is constrained to the p-type bond.

Since this is a fundamental problem of chemical bonding, it is important to attach the different σ^* bonding capacities to some simple property of the atoms C vs Si. This seems to be related to the atomic electronegativities. Indeed in the σ^* of CH_3 the coefficients on C and H are nearly balanced, and the resulting σ^*–S_{ax} overlap is therefore close to zero. On the other hand, the $\sigma^*(SiH_3)$ orbital is more concentrated on the Si atom. This and the long equatorial Si–H bonds cause the σ^*–s_{ax} overlap to be significant.[30]

An important point to make is that the excess bonding in SiH_5^- is *not* a "hypervalency" in the sense of 10 e-bonding. Thus, by mixing structures **1–3** with **4**, SiH_5^- augments its axial bonding at the expense of some weakening of its equatorial bonding. This is done by delocalizing the negative charge on the axial as well as the equatorial bonds, mediated by participation of the equatorial $\sigma^*(SiH_3)$ orbital in bonding. There is thus an energy lowering associated with electronic delocalization. In CH_5^- on the other hand, the mixing of **4** is inefficient, and the excess electrons remain localized in the axial bond. The delocalization option cannot materialize because the $\sigma^*(CH_3)$ orbital does not possess an overlap capability with the axial hydrogens.

B. Geometric Features of CH_5^- and SiH_5^-. As there are two axial bonds in **4** vs only one in **1** or **2**, one expects the axial bond lengths in SiH_5^- to be close to the bond lengths of SiH_4, and those of CH_5^- to be quite stretched relative to CH_4, because structure **4** is important in SiH_5^- and negligible in CH_5^-.

Another expected consequence of the importance of structure **4** is a relatively long Si–H_{eq} bond in SiH_5^-, as compared to a normal Si–H bond. If we consider the orbital occupancy of the central SiH_3 fragment by itself, then within structure **4** this occupancy is $p^1\sigma^{*1}$ (consult **9**). On the other hand, within structures **1–3**, the SiH_3 fragment is in a ground local configuration, with p^1 or p^2 occupancies and an unoccupied σ^* orbital. Therefore, by studying the bond lengths of SiH_3 in the above occupation types ($p^1\sigma^{*1}$ and, e.g., p^2), it is possible to rationalize the SiH_{eq} bond lengths in SiH_5^-, in terms of the weights of the contributing configurations, **1–4**. Indeed, the 6-31G*+D bond length of SiH_3^- (D_{3h}) in a triplet $p^1\sigma^{*1}$ configuration is 1.679 Å, vs 1.480 Å for SiH_3^- (D_{3h}) in its ground state. The Si–H_{eq} bond length in SiH_5^- should accordingly get longer than a normal Si–H bond and should lie in between the limits 1.480 and 1.679 Å. By taking into account the weight (40%) of structure **4** in SiH_5^- and the Si–H stretching force constants for the various orbital occupancies of SiH_3^- (2.08 hartrees/Å^2 for p^2 and 0.93 Å^2 for $p^1\sigma^{*1}$), one can estimate[31] a Si–H_{eq} bond length of 1.529 Å for SiH_5^-, in reasonable agreement with the SCF value in the same basis set. Thus, it appears that the geometric features of SiH_5^- are coherent with an important participation of structure **4**.

C. The σ^* Bonding Capabilities in MO vs VB Theories. The role of $\sigma^*(MH_3)$ orbitals in the bonding features of MH_5^- can be analyzed also in MO terms.[32] Thus, a simple orbital interaction diagram using the orbitals of MH_3 and the symmetry adapted orbitals of H_r and H_l in Figure 2 will reveal that $\sigma^*(SiH_3)$ is more

(30) For such an electronegativity effect consult: Albright, T. A.; Burdett, J. K.; Whangbo, M. H. *Orbital Interactions in Chemistry*; Wiley-Interscience: New York, 1985; pp 18–21.

(31) Calling w_1 and w_2 the respective weights of the p^2 and $p^1\sigma^{*1}$ states of SiH_3^-, k_1 and k_2 their Si–H force constants, and r_{01} and r_{02} their equilibrium Si–H bond lengths, a quadratic expansion of the energy of SiH_3^- is the following: $E = 0.5w_1k_1(r - r_{01})^2 + 0.5w_2k_2(r - r_{02})^2$ + resonance energy due to mixing of structure **4** with **1–3**. Minimizing E with respect to r, the actual Si–H bond length, and neglecting the dependence of the resonance energy on r leads to $\delta E/\delta r = w_1k_1(r - r_{01}) + w_2k_2(r - r_{02}) = 0$, which yields the value $r = 1.529$ Å, to be compared to the SCF value 1.517 Å for SiH_5^-, as computed in 6-31G*+D basis set.

(32) For qualitative MO analyses of pentacoordination in main group elements see: (a) ref 30, pp 273–274. (b) Hoffmann, R.; Howell, J.; Muetterties, E. L. *J. Am. Chem. Soc.* **1972**, *94*, 3047.

Table IV. Coefficients in the HOMO's of the CH_5^- and SiH_5^- Complexes with the Core Atomic Orbitals Omitted

	CH_5^-		SiH_5^-	
	6-31G+D	6-31G*+D	6-31G+D	6-31G*+D
central atom				
inner s	0.1418	0.1347	−0.0362	−0.0010
outer s	0.0417	0.0700	0.2094	0.0383
d		0.0444		0.1619
equatorial H				
inner s	0.0659	0.0581	0.1320	0.1717
outer s	0.1732	0.1616	0.2858	0.2561
axial H				
inner s	−0.2052	−0.2087	−0.2101	−0.2075
outer s	−0.4072	−0.4029	−0.5386	−0.4439
diffuse s	−0.2945	−0.2890	−0.0877	−0.1022

accessible for mixing than $\sigma^*(CH_3)$. As a result the HOMO of SiH_5^- should contain more $\sigma^*(MH_3)$ character than the HOMO of CH_5^-. It is expected accordingly that in comparison with HOMO(CH_5^-), HOMO(SiH_5^-) will involve smaller coefficients on the central atom and larger coefficients on the equatorial hydrogens. The calculated orbitals in Table IV show the latter effect but are not clear for the former. The total effect of $\sigma^*(MH_3)$ mixing is certainly spread over the two a'_1 orbitals of MH_5^-, and it is therefore not easy to reconstruct an argument based on one orbital alone.

There should be no contest between MO and VB; one should be preferred over the other depending on the insight they provide in each specific problem. We think that, in the present problem, the VB treatment in terms of the avoided-crossing diagrams (Figures 3-5) provides insight into the relative stability of SiH_5^- and CH_5^- in a manner that is vivid and instructive. Moreover, on the basis of the bonding descriptions of these species in **9-11**, it is apparent that the qualitative Si-C difference should highly depend on electron count. Thus, removal of one electron will generate the 9-electron species $SiH_5^\bullet$ and $CH_5^\bullet$, which according to **9-11** should both involve a single bond pair of the p-type and behave qualitatively the same. Indeed, both $SiH_5^\bullet$ and $CH_5^\bullet$ are *transition states* along the $H_l + MH_3H_r \rightarrow H_lMH_3 + H_r$ reaction coordinate.[33] It is not easy to come up with a straightforward MO explanation (e.g. based on the HOMOs) of this change upon removal of one electron from the system.

(33) Maitre, P.; Pelissier, M.; Volatron, F. 6-31G*-MP2//6-31G*-MP2 results, manuscript in preparation.

Summary

The qualitative difference between CH_5^- and SiH_5^- is studied by VB computations of avoided-crossing diagrams.[11-19] The diagrams reveal that the stability and compact geometry of SiH_5^- (percentagewise relative to SiH_4) originate in a VB configuration which falls (Figures 4 and 5) below the two classical Lewis structures. This VB configuration involves two axial Si-H_{ax} bonds: one utilizes silicon's axial p-AO and the other utilizes the $\sigma^*(SiH_3)$ orbital. Thus, SiH_5^- lowers its energy relative to its parent fragments (H^-/SiH_4) by delocalizing the fifth valence electron pair into the equatorial Si-H bonds.

In the case of CH_5^-, the diagram (Figure 3) shows that the bonding primarily arises from the avoided crossing of two classical Lewis structures. This produces a high-energy transition state, which possesses a resonating single four-electron/three-center H_{ax}--C--H_{ax} bond. The axial linkages are therefore long relative to the equatorial bonds, and the fifth valence electron pair is localized in the axial portion of the trigonal-bipyramidal structure.

The difference between SiH_5^- and CH_5^- is related to the electropositivity of Si relative to C. This factor endows the $\sigma^*(SiH_3)$ orbital with a bonding capability: low p $\rightarrow \sigma^*$ promotion energy and ability to sustain a high overlap with H_{ax}. This same factor deprives $\sigma^*(CH_3)$ from such capability. Clark[34] has invoked similar overlap arguments to explain the stability of the 9-valence-electron SiH_3Cl^- species, relative to the dissociative behavior of the analogous CH_3Cl^- species. Arguments of another type have been used by Gronert, Glaser, and Streitwieser[35] to explain the stability of SiH_4F^-. Using integrated projection populations, these authors find the silicon atom to have considerable ionic character in this complex and conclude that its stability arises from ionic contributions. We do not think, however, that such an explanation can be extended to the SiH_5^- case, since the ionic contributions are included, within our calculation, in the Lewis structures **1** and **2**, which yield a barrier and not a stable intermediate.

Registry No. SiH_5^-, 41650-16-2; CH_5^-, 12316-54-0.

(34) Clark, T. *J. Chem. Soc., Chem. Commun.* **1981**, 515.
(35) Gronert, S.; Glaser, R.; Streitwieser, A. *J. Am. Chem. Soc.* **1989**, *111*, 3111.

Investigation by MCD of the Low-Lying Electronically Excited States of Some Selected Quinoid Diones

J. Frei, H. Yamaguchi,† J. Tsunetsugu,‡ and G. Wagniere*

Contribution from the Institute of Physical Chemistry, Winterthurerstrasse 190, CH-8057 Zurich, Switzerland. *Received September 16, 1988*

Abstract: The MCD spectra of some quinoid dicarbonyl compounds of pseudoaromatic or antiaromatic character have been recorded. These spectra, combined with calculations of the *B*-terms by the PPP method, provide a detailed analysis of the long wavelength $\pi\pi^*$ bands. Some transitions show a marked charge-transfer character. In one compound we believe to have identified the *A*-term of the $S_0 \rightarrow T_1(^3\pi\pi^*)$ transition.

1. Introduction

In a previous investigation,[1] hereafter designated as I, the long wavelength MCD spectra of some simple *o*- and *p*-quinones have been examined. It has been shown that the signals due to the lower $\pi\pi^*$ transitions in the near-UV may be well-interpreted by the PPP model. The spectra in conjunction with calculations, give information on the polarization of the corresponding bands. The much weaker MCD signals due to the $n\pi^*$ transitions were identified with the help of CNDO calculations. A very weak long wavelength *A*-term appearing in the spectra of some of the com-

* Author to whom correspondence should be addressed.
† Permanent address: Ibaraki University, College of Technology, 4-12-1 Nakanarusawa, Hitachi 316, Japan.
‡ Permanent address: Department of Chemistry, Faculty of Science, Saitama University, Urawa, Saitama 338, Japan.

(1) Meier, A. R.; Wagnière, G. H. *Chem. Phys.* **1987**, *113*, 287.

0002-7863/90/1512-1413$02.50/0